Near-Field Scattering of Typical Targets Illuminated by Vortex Electromagnetic Waves

Hai-tao Chen [1], Ze-qi Zhang [1], and Jie Yu [2]

[1] Department of Antenna Research
Wuhan Maritime Communication Research Institute, Wuhan, 430079, China
hbcht@163.com, zhangzq0812@163.com

[2] Department of Science and Technology
Wuhan Maritime Communication Research Institute, Wuhan, 430079, China
43704378@qq.com

Abstract ─ Based on the full-wave electromagnetic simulation and the principle of near-field diagnostics, the near-field scattering characteristics of typical scatterers illuminated by vortex electromagnetic waves are studied. It's shown from the simulation data that the ability of identification of scatterer characteristics by vortex electromagnetic wave is higher. In addition to the amplitude and phase patterns, the orbital angular momentum (OAM) modal spectrum patterns of the scattering field also carry the information of the geometric shape and material characteristics. The application of OAM modal spectrum patterns will help to improve the ability of information acquisition and target detection of electromagnetic wave.

Index Terms─ Near-field scattering, OAM modal spectrum, vortex electromagnetic wave.

I. INTRODUCTION

Electromagnetic theory shows that electromagnetic (EM) wave can carry not only linear momentum, but also angular momentum. Angular momentum can be divided into spin angular momentum (SAM) and orbital angular momentum (OAM). SAM corresponds to the polarization of EM wave, and OAM depends on the phase structure of EM wave front, which describes the transverse vortex modes of helical beam. Vortex EM wave is a kind of wave with non-zero mode OAM. There is $\exp(jl\varphi)$ phase factor in the field expression of the vortex EM wave, in which φ is the azimuth angle around the propagation direction, and l is the OAM mode number, also known as the topological charge. Theoretically, there are infinite OAM modes for the vortex EM wave. These OAM modes are orthogonal and completeness, constituting an infinite dimension linear space, which is called as OAM modal spectrum domain. Using OAM modal spectrum characteristics to enhance the information transmission, acquisition and target detection has become a very attractive research direction in the field of microwave communication, radar detection and target recognition [1-3].

Scattering characteristics of vortex EM waves are of great scientific significance in both information transmission and information acquisition. For information transmission, due to the influence of space environment, complex effects such as dispersion loss, reflection, refraction, fading and multipath will occur during the propagation of vortex EM wave, which leads to the distortion of vortices and the coupling between OAM modes. The interaction between the vortex EM wave and various obstacles in the propagation process can be attributed to the scattering effect. For information acquisition, the study of electromagnetic scattering characteristics is the basis of radar detection and recognition.

Because of the potential of vortex EM waves in radar imaging, recently some research groups have published research work on radar imaging technology based on the OAM characteristics, trying to improve the resolution of radar imaging [4-6]. In present research of radar imaging technology based on vortex EM wave, the targets are always simplified as the combination of ideal scattering points, ignoring the phase gradient of the incident wave illuminating on the target. Recent advances have shown that the response of complex targets and ideal scattering points to vortex EM wave is quite different, which is reflected not only in the spatial pattern of scattering field, but also in the OAM modal spectral domain. Zhang et al. published an experimental study on RCS diversity effects of vortex EM wave irradiation on complex targets [7]. The results show that for simple targets, such as metal spheres, the same RCS fluctuation characteristics can be obtained under different modes of vortex EM wave irradiation, but for a slightly complex target such as bi-metallic sphere combination, even if the incident angle is the same, different modes of vortex

EM wave can also obtain different RCS. Tang et al. published the results of scattering characteristics of chaff clouds on vortex EM wave [8]. The results show that for a single small dipole, the scattering is not different from that of the plane wave, but for a cloud composed of a large number of dipoles, the scattered wave has a unique distribution in the OAM modal spectrum domain.

The OAM modal characteristics of vortex EM wave mainly exist in the near field region. With the increase of propagation distance, the OAM modal characteristics will gradually degenerate. Therefore, it is more practical to study the near-field scattering of the vortex EM wave, which may play an important role in target detection and recognition.

Based on the commercial EM simulation software FEKO and the principle of near-field diagnostics, the near-field scattering characteristics of typical scatterers illuminated by vortex EM wave are studied in this paper. The full-wave simulation near-field diagnostics are adopted to extract the scattered near-field in Section II, in which the OAM modal analysis is also presented. Some simulation results are shown in Section III, and Section IV is the conclusion.

II. EXTRACTION OF SCATTERED NEAR-FIELD AND OAM MODAL ANALYSIS

Nayeri, Elsherbeni and Yang proposed a near-field diagnostic method based on full-wave electromagnetic simulation software FEKO for reflect-array antenna analysis [9]. Based on this method, the scattered near-field of target illuminated by vortex EM wave is extracted. The process is as follows:

a) Establish the model of the vortex EM wave transmitting antenna in FEKO. In this paper, the circular phased dipole array is used as the transmitting antenna. The radiation field of the transmitting antenna on the scattering field sampling plane is simulated and recorded as the incident field $\mathbf{E}_i$.

b) Establish the model of the transmitting antenna and scatterer in FEKO. The field intensity on the scattering field sampling plane is simulated and recorded as the total field $\mathbf{E}_t$.

c) Read the incident field and total field data by a Matlab code, and subtract the incident field from the total field, then get the scattering field $\mathbf{E}_s$:

$$\bar{E}_s = \bar{E}_t - \bar{E}_i . \tag{1}$$

The phase gradient method has been proposed to detection the OAM mode, in which the signal phases received by two antennas are compared [10]. However, the scattered near-field by complex object illuminated by OAM wave has disorderly phase distribution. The calculated OAM mode spectrum will be depended on the position of the receiving antennas. In order to achieve a comprehensive spectrum analysis of the scattered near field, an aperture integral approach is proposed in this paper based on the orthogonality of the OAM mode. Assuming an imaginary receiving antenna with aperture S is set to receive the scattering field, the received OAM modal spectrum can be calculated as the following formula:

$$P(l) = \frac{1}{A_s} \int_S E_s(x, y) e^{-jl\varphi} dxdy , \tag{2}$$

where l is the OAM mode number, S is the receiving antenna aperture, defined as a circular area of radius [0, R] and angle [0, 2π], A_s is area of the receiving aperture. φ is the phase angle of the complex number $x+jy$. The scattering field data obtained by FEKO software is sampled on rectangular grid, so the OAM modal spectrum can be expressed as a summation form:

$$P(l) = \frac{1}{N_s} \sum_{(m,n)\in S} E_s(m,n) e^{-jl\varphi_{mn}} , \tag{3}$$

where N_S is the number of sampling points falling into the receiving aperture range.

A slotted conductor plate which had been simulated and measured in Ref. [11] is used in this paper as an illustration to check the near-field diagnostic process based on FEKO simulation.
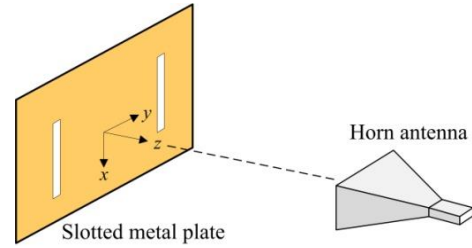
Fig. 1. Illustration example for determining the surface scattered magnetic field on a slotted metal plate illuminated by a horn antenna.

The checking illustration is shown in Fig. 1, in which a metal plate containing two slots is illuminated by a horn antenna. According to Ref. [11], the size of the plate is 30.5cm×30.5cm×0.31cm, and the two slots are 20cm×3.8cm and located symmetrically about the plate center with a distance 11.1cm. The distance between the slotted plate and the horn antenna is 107cm. The incident electromagnetic wave is x-polarization and the frequency is 2GHz.

The near-field diagnostics process is used to extract the scattering magnetic field on a sampling plane which is at the distance 1.27cm from the slotted plate. In order to compare it with the measured data, the "back-propagation approach" [11] is adopted to transform the magnetic field on the sampling plane to on the slotted plate. The normalized scattered magnetic field is shown in Fig. 2, which is in good agreement with the measured data presented in Ref. [11].

In order to check the OAM spectrum analysis method, the spectrum of a vortex EM wave with noninteger OAM state is examined by the aperture integral approach and the Fourier series method [10, 12] respectively. The mode number of the incident wave is set to 0.5. The radius of the receiving aperture is $2\lambda_0$ and the sample spacing is $0.1\lambda_0$. The spectrum patterns of the two methods are accordant, as shown in Fig. 3.

(a)

(b)
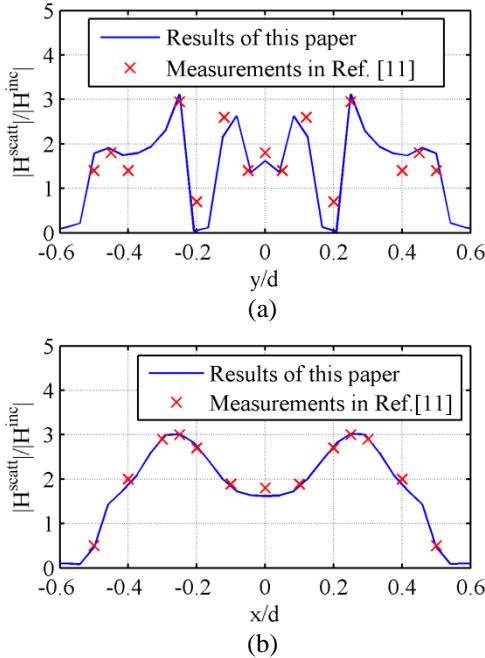
Fig. 2. Normalized scattered magnetic field on the slotted plate. Incident electric field is parallel to the slots. (a) Cross section of the magnetic field in the y-direction, and (b) x-direction are shown.
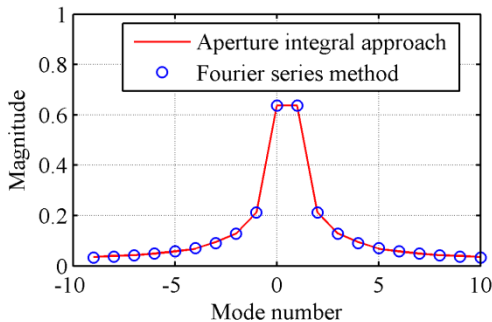
Fig. 3. OAM spectrum of the vortex EM wave with OAM mode l=0.5.

III. SIMULATION EXAMPLES

A. Scattering of PEC plates

The circular four-element phased array is used as the vortex EM wave transmitting antenna. The radius of the array is $1\lambda_0$ and the radiated electric field is x-polarized. As shown in Fig. 4, a $10\lambda_0\times10\lambda_0$ rectangular PEC plate is symmetrically placed on the propagation axis of the transmitting beam, $30\lambda_0$ away from the transmitting array. Based on the simulation results of FEKO software, the scattering field is extracted by using the near-field diagnostics method. The scattering field sampling plane is $10\lambda_0$ away from the plate. Figure 5 shows the amplitude and phase pattern of the x-polarization scattering field and the OAM modal spectrum. When calculating the OAM modal spectrum, the receiving aperture is a circle with radius of $1\lambda_0$. Figure 5 (a) shows the magnitude of the scattering field, from which the edge of the plate can be roughly seen. The phase pattern shows that the scattering field of the conducting plate is still a vortex EM wave with first order OAM. Figure 5 (c) shows the mode spectrum of the scattering field, which confirms that the first order mode is still dominant.
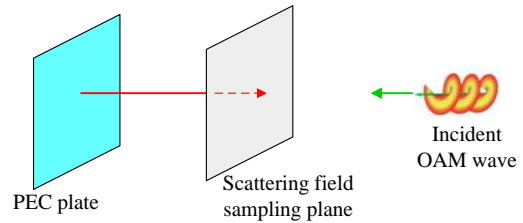
Fig. 4. Scattering of the OAM waves by a PEC plate.

(a) (b)

(c)
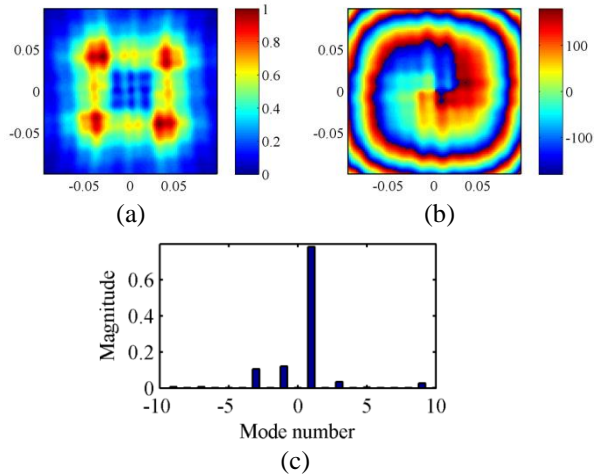
Fig. 5. Backscattering field of the PEC plate illuminated by the OAM wave with l=1. (a) Amplitude, (b) phase, (c) modal spectrum. The plate is placed symmetrically perpendicular to the axis of the OAM wave, $30\lambda_0$ from the transmitting antenna array, $10\lambda_0$ from the scattering field sampling plane.

If the transmitting antenna is fed in-phase, the OAM modulus of the transmitting beam is turn to zero. Figure 6 shows the amplitude, phase and mode spectrum patterns

of the scattering field. Compared with Fig. 5, it can be seen that the vortex EM wave with OAM mode number $l=1$ has better identification ability for the edges and corners of the plate. Note that the mode spectrum magnitude in Fig. 5 (c) is much smaller than that in Fig. 6 (c). It can be attributed to the amplitude nulls in the beam direction for OAM wave.

(a)   (b)

(c)
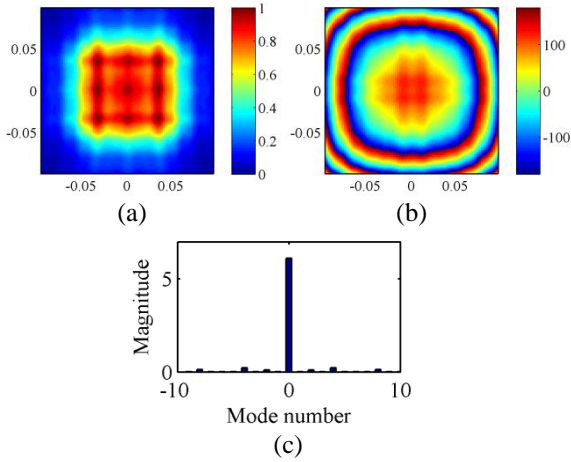
Fig. 6. Backscattering field of the PEC plate illuminated by the OAM wave with $l=0$. (a) Amplitude, (b) phase, and (c) modal spectrum. The plate is placed symmetrically perpendicular to the axis of the OAM wave, $30\lambda_0$ from the transmitting antenna array, $10\lambda_0$ from the scattering field sampling plane.

(a)   (b)

(c)
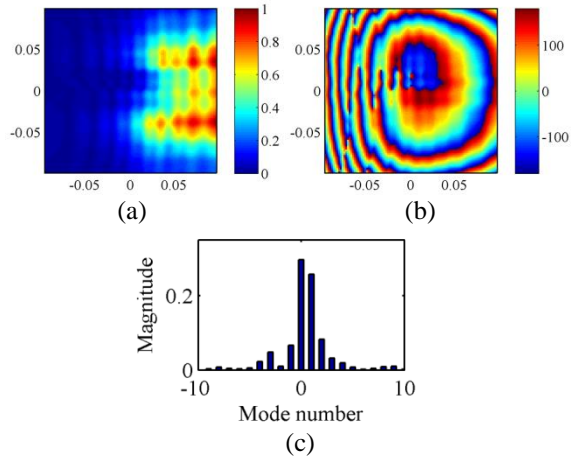
Fig. 7. Backscattering field of the PEC plate illuminated by the OAM wave with $l=1$. (a) Amplitude, (b) phase, and (c) modal spectrum. The plate is placed perpendicular to the axis of the OAM wave and deviates from the axis by $5\lambda_0$, $30\lambda_0$ from the transmitting antenna array, $10\lambda_0$ from the scattering field sampling plane.

It can be seen from Fig. 5 that the scattering field of the PEC plate arranged axially symmetrically along the vortex EM wave propagating axis maintains the OAM

mode spectrum of the incident wave well. Now the plate is shifted $5\lambda_0$ perpendicular to the axis of the OAM wave. Then the vortex EM wave illuminating on the plate will no longer have a complete phase gradient distribution. It can be predicted that the scattering field will no longer have a simple first-order OAM mode. The simulation data shown in Fig. 7 verifies it. It can be seen that besides the first-order OAM, the 0-order OAM component in the scattering field is also stronger.

B. Scattering of cones

The scattering of OAM waves by a conducting cone is investigated, as shown in Fig. 8. The diameter of the conical surface is $10\lambda_0$ and the height is also $10\lambda_0$. The conical axis coincides with the propagation axis of the vortex EM wave. The top of the cone points to the transmitting antenna at a distance of $30\lambda_0$. The sampling plane of the scattering field is $10\lambda_0$ from the top of the cone.
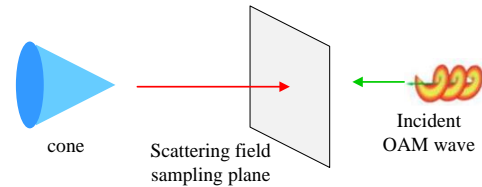
Fig. 8. Scattering of the OAM waves by a cone.

Similarly, a four-element circular phased array is used as the vortex EM wave transmitting antenna. The amplitude and phase patterns of the scattering field on the sampling plane are shown in Fig. 9. From the phase pattern, it can be seen that in a small area around the center, the scattering field still has good first-order OAM characteristics, but in other areas, the spiral phase distribution has not been seen. Figure 10 shows the OAM modal spectrum obtained from different receiving apertures. It can be seen that when the receiving aperture exceeds the radius of the bottom of the cone, the high-order OAM mode will increase significantly.

(a)   (b)
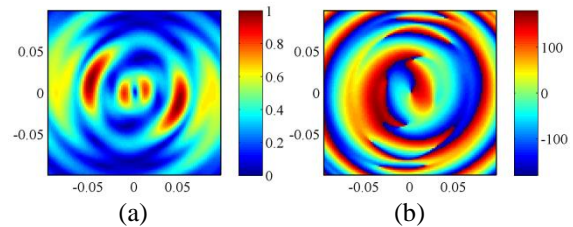
Fig. 9. Backscattering field of PEC cone illuminated by the OAM wave with $l=1$. (a) Amplitude and (b) phase.

Replaced the PEC cone by a dielectric cone with same size and the dielectric constant is $\varepsilon_r=4.0$. Figure 11 shows the scattering field on the sampling plane when the incident wave is first-order OAM and 0-order OAM,

respectively. The receiving aperture is a circle with radius of $2\lambda_0$. It can be found that the vortex EM wave has higher recognition ability for conical vertices. Besides the amplitude and phase, the OAM modal spectrum pattern also reflects the characteristic information of scatterers. Compared with the PEC conical scattering, the bottom edge diffraction effect of the dielectric cone is obviously weakened, and the parasitic OAM mode l=-1 is enhanced.
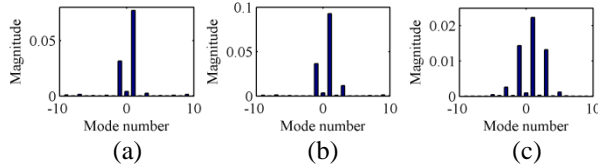
Fig. 10. OAM modal spectrum patterns of the scattering field of the PEC cone illuminated by OAM wave with l=1. Receiving aperture radius: (a) R=λ_0; (b) R=$2\lambda_0$; (c) R=$5\lambda_0$.
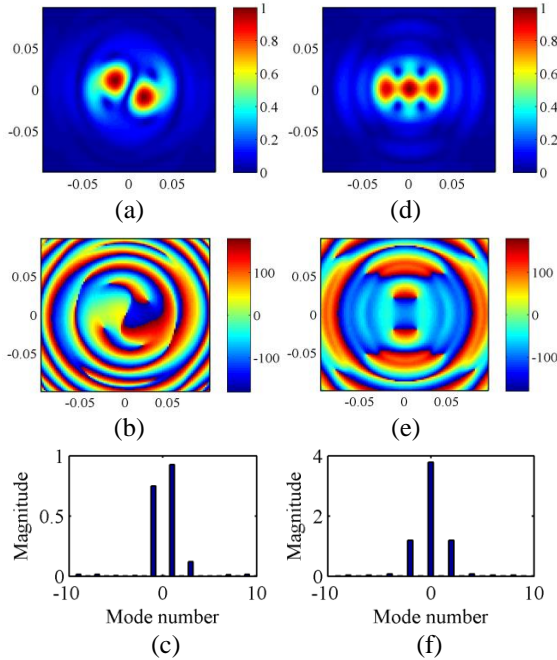
Fig. 11. Scattering field of the dielectric cone illuminated by OAM wave. (a) Amplitude, (b) phase, and (c) modal spectrum for the incident wave with OAM mode l=1. (d) Amplitude, (e) phase, and (f) modal spectrum for the incident wave with OAM mode l=0.

C. Scattering of two metal spheres

A case of scattering of vortex EM wave from multi-targets is investigated. As shown in Fig. 12, two metal spheres with radius $2.5\lambda_0$ and distance $10\lambda_0$ are symmetrically placed on the propagation axis of the transmitting beam, $30\lambda_0$ away from the transmitting array. The spheres are illuminated by a twelve-element

circular phased array. The radius of the array is $1.5\lambda_0$. The OAM mode of the transmitting is set to 0, 1, 2 and 3 respectively. The amplitude, phase and OAM modal spectrum pattern of the scattering field are shown in Fig. 13, in which the receiving aperture is a circle with radius of $5\lambda_0$. The sampling plane of the scattering field is $10\lambda_0$ away from the center of the spheres.
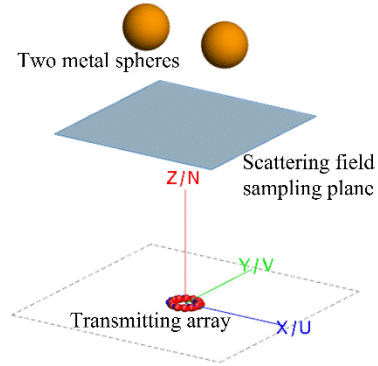
Fig. 12. Two metal spheres illuminated by OAM circular phased array.
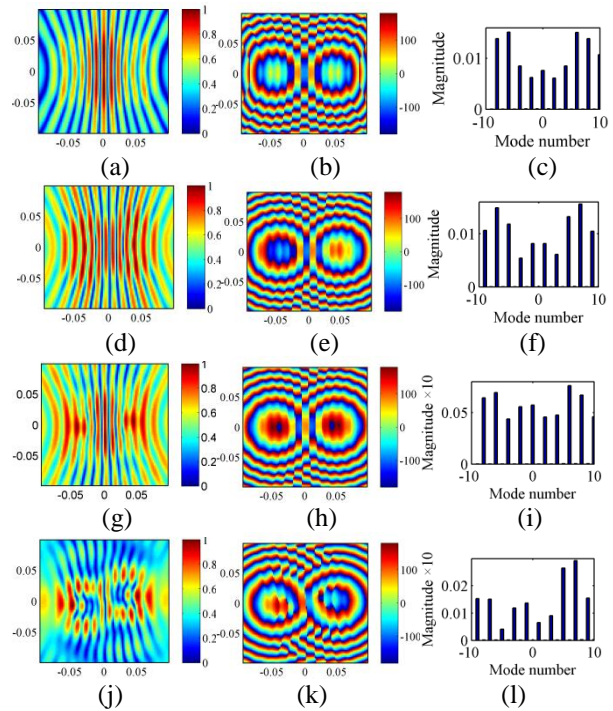
Fig. 13. Near scattering field by two spheres illuminated by OAM wave with different mode. (a) Amplitude, (b) phase, and (c) modal spectrum for the incident wave with OAM mode l=0. (d) Amplitude, (e) phase, and (f) modal spectrum for the incident wave with OAM mode l=1. (g) Amplitude, (h) phase, and (i) modal spectrum for the incident wave with OAM mode l=2. (j) Amplitude, (k) phase, and (l) modal spectrum for the incident wave with OAM mode l=3.

The interference fringes can be clearly observed from the simulated results. It is caused by the interference of two metal spheres scattering field. The position of two metal spheres can be clearly judged from the phase pattern of the scattering field. Since the target no longer has axisymmetric properties, there are many higher order modes in the OAM spectral domain of the scattering field. It can be found that when the mode of incident wave OAM is $l=0$ and $l=2$, the mode spectrum of scattering field OAM is similar, which can be explained as the incident wave of mode $l=0$ and $l=2$ has the same phase on the centers of the two spheres.

IV. CONCLUSION

It is demonstrated that the scattering field of different targets illuminated by OAM wave does not only show the spatial distribution of amplitude and phase, but also exhibit unique distribution characteristics in the OAM modal spectrum domain. Through the interaction between the vortex EM wave and the target, more target information can be obtained from the echo signal, which provides a new technical way for target detection and recognition.

REFERENCES

[1] L. Allen, M. W. Beijersbergen, R. J. C. Spreeuw, and J. P. Woerdman. "Orbital angular momentum of light and the transformation of laguerre-gaussian laser modes," *Phys. Rev. A*, 45, 8185, 1992.

[2] B. Thide, et al., "Utilization of photon orbital angular momentum in the low-frequency radio domain," *Phys. Rev. Lett.*, 99, 087701, 2007.

[3] F. Tamburini, et al., "Encoding many channels on the same frequency through radio vorticity: First experimental test," *New J. Phys.*, 14, 033001, 2012.

[4] K. Liu, Y. Cheng, Z. Yang, H. Wang, Y. Qin, and X. Li, "Orbital-angularmomentum-based electro-magnetic vortex imaging," *IEEE Antennas Wireless Propag. Lett.*, vol. 14, pp. 711-714, 2015.

[5] B. Tang, K.-Y. Guo, J.-P. Wang, et al., "Orbital-angular-momentum-based imaging radar," *IEEE Antennas and Wireless Propagation Letters*, vol. 16, pp. 2975-2978, 2017.

[6] X. Bu, Z. Zhang, L. Chen, et al., "Implementation of vortex electromagnetic waves high-resolution synthetic aperture radar imaging," *IEEE Antennas And Wireless Propagation Letters*, vol. 17, no. 5, pp. 764-767, 2018.

[7] C. Zhang, D. Chen, and X. Jiang, "RCS diversity of electromagnetic wave carrying orbital angular momentum," *Scientific Reports*, 7: 15412 doi:10. 1038/s41598-017-15250-7, 2017.

[8] B. Tang, J. Bai, and X.-Q. Sheng, "Orbital angular momentum carray wave scattering by the chaff clouds," *IET Radar, Sonar and Navigation*, vol. 12, no. 6, pp. 649-653, 2018.

[9] P. Nayeri, A. Z. Elsherbeni, and F. Yang, "Design, full-wave analysis, and near-field diagnostics of reflectarray antennas," *ACES Journal*, vol. 28, no. 4, pp. 284-292, Apr. 2013.

[10] K. Liu, H. Liu, Y. Qin, et al., "Generation of OAM beams using phased array in the microwave band," *IEEE Trans. Antennas Propagat.*, vol. 64, no. 9, pp. 3850-3857.

[11] P. H. Harms, J. G. Maloney, M. P. Kesler, E. J. Kuster, and G. S. Smith, "A system for unobtrusive measurement of surface currents," *IEEE Trans. Antennas Propagat.*, vol. 49, pp. 174-184, Feb. 2001.

[12] F. Tamburini, E. Mari, B. Thidé, C. Barbieri, and F. Romanato, "Experimental verification of photon angular momentum and vorticity with radio techniques," *Appl. Phys. Lett.*, vol. 99, no. 20, p. 204102, 2011.